Asian Journal of Water, Environment and Pollution, Vol. 19, No. 1 (2022), pp. 59-65.
DOI 10.3233/AJW220009

Prediction of Fractures and Cracks to Improve the Drilling Operations

Saade Abdalkareem Jasim*, Khaldoon T. Falih[1], Ahmed Kateb Jumaah Al-Nssairi[2], Ola Kamal A. Alkadir[3], Yasser Fakri Mustafa[4] and Li Yang[5]

Medical Laboratory Techniques Department, Al-maarif University College, Al-anbar-Ramadi, Iraq
[1]New Era and Development in Civil Engineering Research Group, Scientific Research Center, Al-Ayen University, Thi-Qar, Iraq
[2]Al-Manara College For Medical Sciences, Iraq
[3]Al-Nisour University College, Baghdad, Iraq
[4]Department of Pharmaceutical Chemistry, College of Pharmacy, University of Mosul, Mosul – 41001, Iraq
[5]School of Civil Engineering, Beijing Jiaotong University, Beijing, China
✉ saade.a.j@uoa.edu.iq

Received March 6, 2021; revised and accepted April 26, 2021

Abstract: The term fracture is defined in different ways in geology; some definitions have a defining aspect, while other definitions have dealt with this issue in more detail. There may be differences in appearance and strength that distinguish them from each other, generally in the drawings of an illustrator diagram. According to electrical logs such as formation micro-imager (FMI), fractures are seen in three vertical fractures, polygonal fractures and mechanical fractures. In this paper, different types and methods of diagnosis of each fracture were evaluated. Moreover, by showing examples of these fractures, especially mechanical fractures in the FMI tool's images, we become practically acquainted with these construction features. According to the findings of this study, large open cracks cause considerable variations in dense, shear, and columnar values, and large vertical cracks are due to significant differences in shear tension.

Key words: Fracture, FMI, cracks, shear tension.

Introduction

Petrophysics is considered as the study of rock properties and its interaction with fluid, which consists of gas, liquid hydrocarbons, or aqueous solutions (Dhir et al., 2020; Dymond et al., 2013; Egermann et al., 2010; Gholamin & Khayatnezhad, 2020; Jin et al., 2015; Liu et al., 2020; Mohammed & Corbett, 2003; Rücker et al., 2020). Since petroleum reservoir rocks must have proper porosity and permeability, petrophysics further investigates the properties of porous and permeable rocks (Alkawaz et al., 2020; Caubit et al., 2009; Da Silva et al., 2015; Dwijendra, 2020; Jin et al., 2015; Maloney & Briceno, 2009; Movchan et al., 2021). In formations' drilling, identifying valuable hydrocarbon layers from hydrous formations or low porosity determines intervals for well testing essential for engineering purposes (Al-Sanjary et al., 2018; Ghadiri et al., 2014; Worthington, 2010). Fractures are the most common geological structure and can be seen in any rock outcrop (Aydin, 2000; Bjørlykke & Høeg, 1997; Davies et al., 2013; Dmytro, S.T., 2020; Dwijendra et al., 2021; Nygård et al., 2006). Fractures are cracks along which the cohesion of the material decreases and are therefore considered discs or surfaces of discontinuity.

*Corresponding Author

Zhai et al. (2021) developed a numerical model to simulate the induced fracture leakage based on the fracture types. Therefore, the developed dynamic model focussed on the fracture parameter such as fluid viscosity, leakage rate, and wellbore radius. They concluded that leakage pressure had been increased with the increase of induced fracture and fracture width (Zhai et al., 2021). Sabah et al. (2021) proposed a series of algorithms to predict the lost circulation during the fracturing processes. This infers that hybrid intelligent models are considered efficient methods to predict loss circulation (Sabah et al., 2021). Ezati et al. (2018) developed a model to study the prediction of the microfractures in the Sarvak Formation in Iran. Microfractures show that the permeability-porosity trend is not usually through the pore channels (Ezati et al., 2018).

In this study, we aimed to present different imaging logs and microfractures prediction tools to define the heterogeneity of the porous media. Moreover, the crucial factors that affect the logging tools, such as fracture morphology and fracture distancing, have been investigated.

Methods

In water-based drilling mud, formation micro-imager (FMI) should be used, while in oil-based drilling mud, two complimentary logs, oil base mud illustrator (OBMI) and ultrasonic well wall illustrator (UBI) should be used. In general, OBMI is suitable for determining the characteristics of sedimentary structures, and UBI is suitable for determining cracks and well stability. In any reservoir, it is essential to identify the cracks and the direction of the cracks. One of the applications of imaging is to determine the location of cracks. Over the years of literature surveys, we have evaluated the reservoir cracks imaging, which explain how different images are affected by the presence of cracks and how these cracks can be identified. In this study, we have tried to introduce most of the methods for identifying and detecting cracks. FMI logs are shown in Figure 1.

Identification of Cracks by Acoustic Imaging Logs

As the curve of the acoustic diagram is relatively smooth in most parts of the open well, there are some distorted parts at some other distances. The part of the

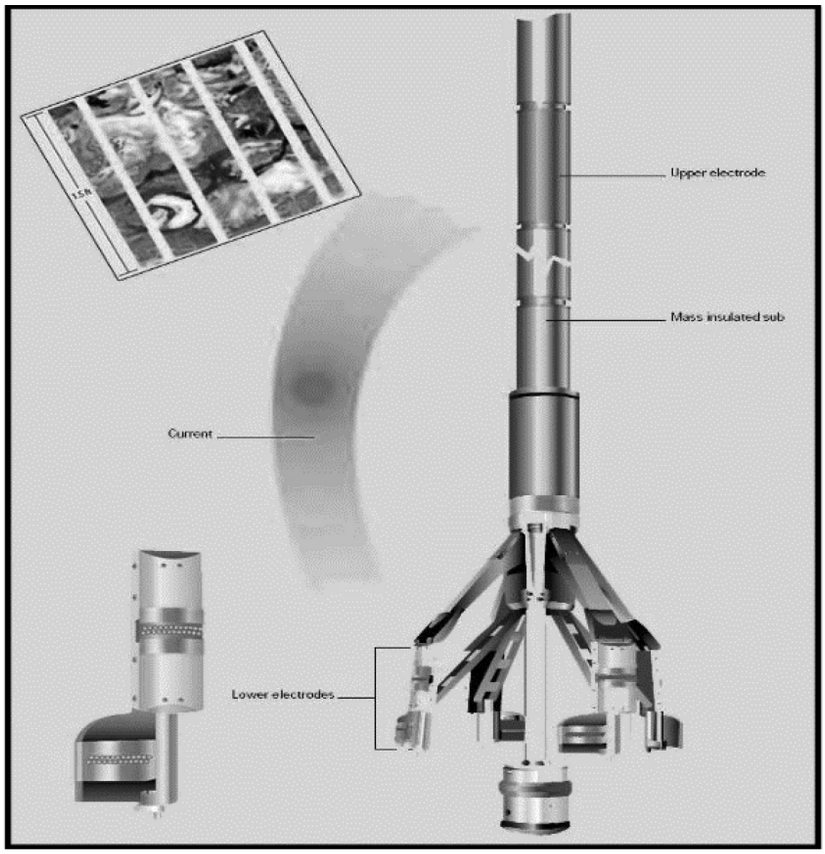

Figure 1: FMI tools with the sensors.

caliper that is irregular and distorted can be evidence of a crack because the fluid inside the cracks will prevent the passage of acoustic signals. The caliper measures the four-diagonal acoustic log, which differs depending on those receivers and transmitters affected by the crack. It rotates the log as it ascends changes the effect of the crack from one receiver to another. The FMI log has many applications in reservoir engineering and geology prospects, where this log operates based on resistance. The FMI has four arms, eight pads, and 192 electrodes. In the output diagram of this log, the areas with low resistance will be black. This log can measure cracks quantitatively, detect their direction, and be one of the best and most powerful tools for detecting and identifying cracks.

Resistance Image of Oil Base Mud Illustrator (OBMI) and Ultrasonic Well Wall Illustrator (UBI)

The use of oil-based drilling fluid has significantly reduced the risks of drilling and increased yield strengths. At the same time, new imaging logs should be made using oil-based drilling fluid. Hence, these two logs, OBMI and UBI, were the result of this effort. It is noteworthy that the FMI log can drive in salt formations (non-conductive phase is more than 80%), so if the drilling fluid is oily, a combination of OBMI and UBI logs is preferred. OBMI has four pads and 40 electrodes with a general accuracy of 4.0 inches. There are two electrodes at both ends of each pad that conduct current into the mud. In the middle of this pad, there are two rows of five electrodes in each row. These electrodes measure the potential difference created in the mud by this current. The output of this log, like the FMI log, is such that the high resistance areas are highlighted, and the low resistance areas are marked in dark colours.

Results

Fractures are recognisable by their relative motion along the fracture surfaces of an outcrop formation. Fractures are initially open but may later be filled by various minerals, thus accelerating and modulating the flow of fluids.

Morphology of Fractures

One of the critical factors influencing fractures in porosity and permeability is the morphology of the fracture surface. Examination of the resulting shape can be done by studying cores and outcrops and sometimes using electrical diagrams. There are four basic shapes in fracture surfaces that are schematically depicted in Figure 2. Reconstructive fractures are more conductive than their lateral fractures. The filled type of sediments is less conductive than their recurrent fractures. Semi-closed fractures show an intermediate state between the two groups. Besides, the fracture's conductivity depends on the strength of the mud, the strength of the affected zone, and the geometry of the fracture. A visual inspection of electrical images alone can guide the interpretation of the reservoir.

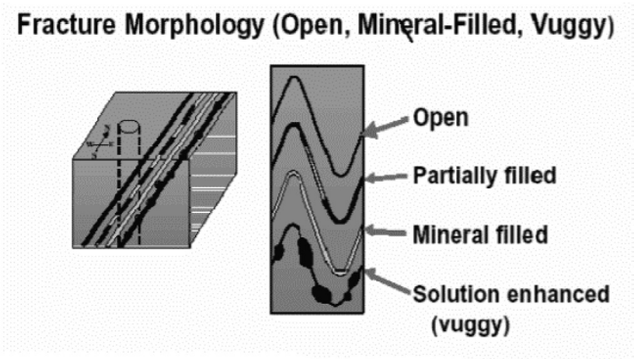

Figure 2: Fracture morphology.

Factors Controlling the Distance Between Fractures in the Basement

According to the information obtained from the interpretation of illustrator diagrams and various experiments, fracture control factors in the formations are rock types, porosity, and particle dimensions. Particle dimensions are controlled by changing the material, and therefore, there is no quantitative relationship between the dimensions of particles and grains formed in the rock and the distances between fractures. In the construction location, there are two methods for determining the density of fractures at this stage. One is to pay attention to stored energy and stress, and the other is to use the radius of curvature or changes in the amount of slope. According to the second method, the assumption of maximum fracture density (short distance between fractures) occurs when changes in the slope of the layer and the radius of curvature are maximum. It was also assumed that the increase causes a mass increase in fractures. The fact that this method is more qualitative than quantitative should not be overlooked.

Pattern of Fractures in Southwestern Iran

Sangree et al. (1961) were the pioneers who examined fractures, whether seams or faults related to their direction along the axis of anticlines and generally divided them into two main and sub-categories. Pattern 1; transverse fractures, pattern 2; longitudinal fractures,

and pattern 3; diagonal fractures. This classification was later replaced by Stearns & Fridman (1972). However, there is no difference between the two classifications as Stearns & Fridman (1972), patterns 1 and 2 are transverse, and Sangree et al. (1961) are longitudinal fractures, respectively. Figure 3 shows a general and symbolic picture of the study of fracture patterns by Stearns & Fridman (1972).

In pattern 1, fractures are usually accompanied by a series of tensile or shear conjugate fractures perpendicular to the floor's surface, respectively, and mainly in the edges. In the case of shear fractures of this pattern, they are thought not to affect the permeability of the rock and are considered by others to be an obstacle in a permeation system. It is shown in Figure 4.

In pattern 2, tensile or shear fractures parallel to the axis of the anticline or make angles of 30 to 35°, respectively. Their region of origin is between the point of the ridge to the place above the turning point—the point where the anticline edge becomes the syncline edge. In any case, group 2 fractures appear in the hinge area and gradually decrease in severity and number towards the lower part of the edges. These fractures are considered due to their effect on reservoir permeability. According to surface studies, the number of longitudinal fractures is four times the transverse type. It is shown in Figure 5.

In pattern 3, tensile fractures with shear have conjugated fracture parallels to the axis of the intersects. The difference between this pattern and the other two patterns is changing the direction of the axis of the maximum principal stress, which occurs perpendicular to the wall of the layer. In terms of location, these fractures are more common in the hinge area.

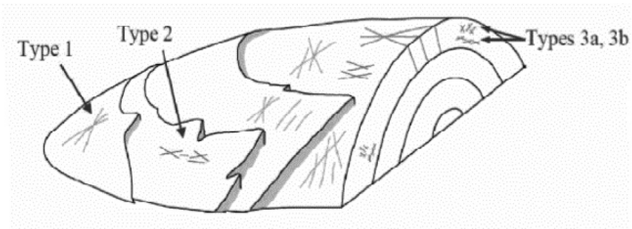

Figure 3: Overview of typical patterns of fractures concerning anticlines quoted.

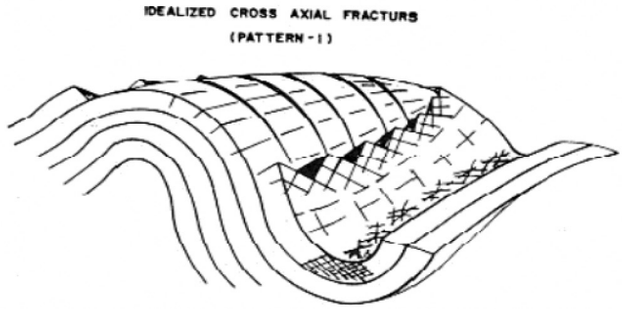

Figure 4: Display of transverse fractures or pattern number one.

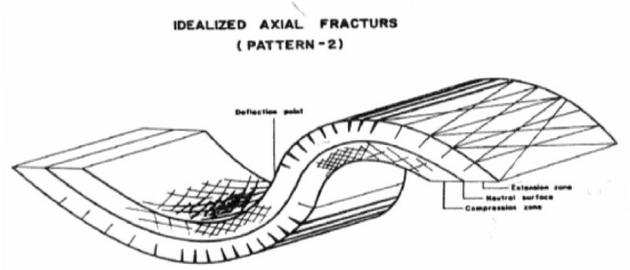

Figure 5: Approximate diagram of longitudinal fracture spread or pattern number 2.

Vertical Fractures

If open fractures filled with minerals, they show relatively good conductivity. Their slope can be oriented using conventional methods. The angular inclination of these fractures controls proper production and recovery capacity in some reservoirs. It is usually based on 75°; fractures with a slope angle of more than 750 are called vertical, and less than 750 are called steep. It is shown in Figure 6.

Mechanical Fractures

They are formed because of processes during drilling (drill blows to the well wall and formation) or a hydraulic fracture (force due to the weight of the drilling fluid). Mechanical fractures occur at different depths in different ways. At shallow depths, the force

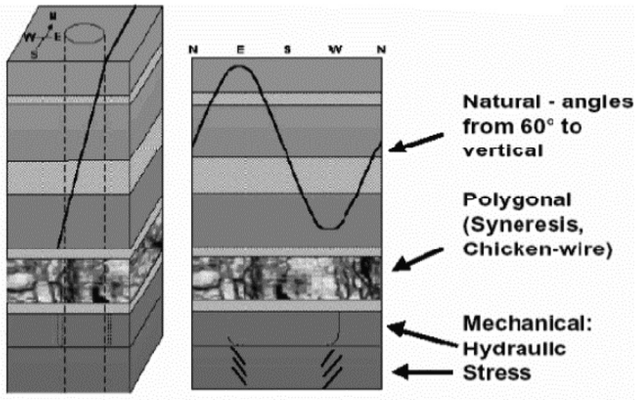

Figure 6: Identification of fractures in electrical diagram drawings.

from overburden pressure (*v*) is less than the horizontal stresses (3, 1) applied to the well. Therefore, the fractures in the well wall will be horizontal. Besides, because the applied force overcomes the minimum available force, the direction of opening of these fractures will be up and down. It is shown in Figure 7.

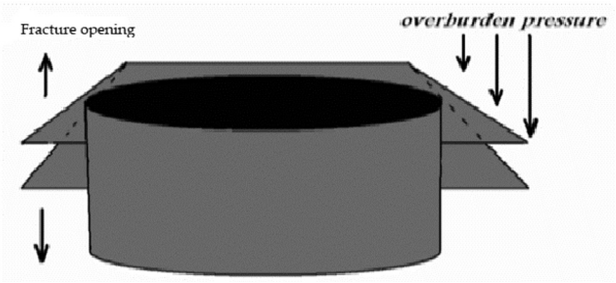

Figure 7: Fracture opening.

At great depths, the force from overburden pressure (*V*) is greater than the horizontal stresses (3, 1) applied to the well. Therefore, the fractures in the well wall will be vertical and in the direction of maximum horizontal stress (1). Also, because the applied force overcomes the minimum available force (minimum horizontal stress), the fractures will be opposite (3).

Analysis of Khami Reservoir Fractures of Chillinger Oilfield Using Core and Illustrator Diagrams

Iran's carbonate reservoirs are of great importance due to having many fractures and the effectiveness of these fractures in oil production. Therefore, determining the density of fractures, the direction of their slope and extension, the number of openings and their distances, or their closure or fullness by different minerals and drawing a suitable pattern of fractures will significantly increase oil production fields. The primary purpose of this study was to accurately determine the number of fractures, slope, direction and extension, an extension of stratification, density, and expansion of fractures in different layers, and their compliance with well hydrodynamic information. Moreover, the determination of fracture zones for further exploitation of layers and determining the direction of stresses on different formations of Khami group (Surmeh, Fahlian, Gadun, and Darian formations) is Chillinger oil field is evaluated. In this study, in order to achieve the above goals, the FMS tool has been used. This tool continuously and partially shows the vertical and lateral changes in the properties of the formation in such a way that the researcher can observe the formation.

Discussion

Several charts can be used to find and detect cracks. Different acoustic techniques between single diagrams will be suitable methods for detecting cracks. The FMI device is a potent tool for identifying gaps. Despite these, other diagrams, such as SP, all resistance devices with shallow depth of field, and gamma-ray spectroscopy can give us more indications in this regard. In the final analysis, the best way is to use and combine several methods to detect cracks for the Khami reservoir. Changes in the height of the waveform may be evidence of the existence of cracks. Changes in apparent velocities will provide important information about the type and size of cracks. The crack's exact height and slope angle can be determined when these differences are combined with Dipmeter and BHTV information. This method is sensitive to cracks produced by cracks, which have a slight sensitivity to the boundary of the layers and can detect cracks by increasing the diameter of the well. Conventional elevation charts will most importantly provide only qualitative information about the cracks if their specificity is desired.

Conclusion

Using a graph alone cannot give us a reliable answer about the distribution and geometry of fractures. However, in any case, each graph is affected by fractures, and important reservoir parameters such as fracture index can be (FI) were well estimated using a combination of well diagrams in broken reservoirs. As a result, no graph alone can be the cause of a fracture. The diagnosis of fractures is more confident when most diagrams and methods confirm their existence. Finally, it should be said that in each location, after studies and tests, the best combinations of diagrams to identify fractures are identified and used in other wells drilled in that area. Because the OBMI log does not cover the entire wall of the well 100%, in order to eliminate this defect, the researchers are trying to place another OBMI catheter at a 45° angle next to an OBMI catheter. In general, in two pieces of rock with a combination of mineralogy and similar texture, less porosity reduces the distance between fractures and vice versa. If we assume that other factors influencing the distance between fractures are constant, thinner layers usually have a shorter distance between fractures.

- Polygonal fractures are multidimensional in appearance in three dimensions because they are

affected by volumetric forces. As a result, polygonal fractures are not orientable.

- Mechanical fractures are generally open fractures and are easily navigable. The method of this group is affected by the maximum horizontal stress.
- In the FML images given in the text, it can be seen that these fractures have spread in a north-south direction, which is in line with the direction of the most horizontal stress. Despite the above, this should be considered from experience as the safest way to diagnose the type of fracture by observing their appearance.
- The fractures seen on the Chillinger 4 well cores are entirely consistent with the fractures resulting from the FMS diagram images' interpretation. Also, the information obtained from the low percentage of core recovery in the Chillinger 7 well is utterly consistent with the images and the spread of fractures resulting from the interpretation of the FMS diagram.
- No significant fractures were observed in the thin microscopic sections studied in Surmeh formation in Chillinger well 7. Most of the fractures in thin sections are related to Fahlian and Gadun Formations.
- According to the bar chart of Chillinger 4 well, complete waste has been done at the base of the Fahlian Formation. The fractures resulting from the interpretation of the FMS diagram are entirely consistent with the waste intervals at these depths. However, in the Chillinger 7 well, the waste does not match the fractures resulting from the interpretation of the FMS diagram.
- A total of 616 discontinuous open fractures generally have two general trends in the formations of the upper crude group (Darian, Gadun, and Fahlian) obtained from interpreting the FMS diagram of the Chillinger 4 well. The first group is transverse fractures with a slope of 78-60° to the north and to 10° west, and the second group of shear fractures with a slope of 82-55° to the north 45° west.

Abbreviations

FMI	Formation Micro-Imager
UBI	Ultrasonic Well Wall Illustrator
OBMI	Oil Base Mud Illustrator

Acknowledgement

Fundamental Research Funds for the Central Universities (2015YJS120)

References

Al-Sanjary, O.I., Ahmed, A.A., Jaharadak, A.A. B., Ali, M.A. and H.M. Zangana (2018). Detection clone an object movement using an optical flow approach. *In 2018 IEEE Symposium on Computer Applications and Industrial Electronics*. (ISCAIE) (pp. 388-394). IEEE.

Alkawaz, M.H., Veeran, M.T. and R. Bachok (2020). Digital image forgery detection based on expectation maximization algorithm. *In 2020 16th IEEE International Colloquium on Signal Processing and Its Applications,* (CSPA) (pp. 102-105). IEEE.

Aydin, A. (2000). Fractures, faults, and hydrocarbon entrapment, migration and flow. *Marine and Petroleum Geology*, **17(7):** 797-814.

Bjørlykke, K. and K. Høeg (1997). Effects of burial diagenesis on stresses, compaction and fluid flow in sedimentary basins. *Marine and Petroleum Geology*, **14(3):** 267-276.

Caubit, C., Hamon, G., Sheppard, A.P. and P.E. Øren (2009). Evaluation of the reliability of prediction of petrophysical data through imagery and pore network modelling. *Petrophysics*. The SPWLA Journal of Formation Evaluation and Reservoir Description, **50(04).**

Da Silva, P.N., Gonçalves, E.C., Rios, E.H., Muhammad, A., Moss, A., Pritchard, T., Glassborow, B., Plastino, A. and R.B.D.V Azeredo (2015). Automatic classification of carbonate rocks permeability from 1H NMR relaxation data. *Expert Systems with Applications*, **42(9):** 4299-4309.

Davies, R., Foulger, G., Bindley, A. and P. Styles (2013). Induced seismicity and hydraulic fracturing for the recovery of hydrocarbons. *Marine and Petroleum Geology,* **45:** 171-185.

Dhir, R., Ashok, M. and S. Gite (2020). An overview of advances in image colorization using computer vision and deep learning techniques. *Review of Computer Engineering Research,* **7(2):** 86-95.

Dmytro, S.T. (2020). The study of welding requirements during construction and installation of seismic-resistant steel structures. *Journal of Research in Science, Engineering and Technology*, **8(2)**.

Dwijendra, N.K.A. (2020). Meru as a hindu sacred building architecture with a high roof and resistant to earthquakes in Bali, Indonesia. *Philosophy,* **16(24):** 46.

Dwijendra, N.K.A., Akhmadeev, R., Tumanov, D., Kosov, M., Shoar, S. and A. Banaitis (2021). Modeling social impacts of high-rise residential buildings during the post-occupancy phase using DEMATEL method: A case study. *Buildings*, **11(11):** 504.

Egermann, P., Bekri, S. and O. Vizika (2010). An integrated approach to assess the petrophysical properties of rocks altered by rock-fluid interactions (CO_2 Injection). *Petrophysics* - The SPWLA Journal of Formation Evaluation and Reservoir Description, **51(01)**.

Ezati, M., Azizzadeh, M., Riahi, M.A., Fattahpour, V. and J. Honarmand (2018). Characterization of micro-fractures

in carbonate Sarvak reservoir, using petrophysical and geological data, SW Iran. *Journal of Petroleum Science and Engineering*, **170:** 675-695.

Ghadiri, M., Khanmohammadi, A., Mahdavi, H.R., Ahmadi, M., Mirzaei, T. and H. Easy (2014). Fracture mechanics analysis of fourth lumbar vertebra in method of finite element analysis. *International Journal of Advanced Biological and Biomedical Research,* **2(7):** 2217-2224.

Jin, X., Shah, S.N., Roegiers, J. C. and B. Zhang (2015). An integrated petrophysics and geomechanics approach for fracability evaluation in shale reservoirs. *SPE Journal*, **20(03):** 518-526.

Maloney, D.R. and M. Briceno (2009). Experimental investigation of cooling effects resulting from injecting high pressure liquid or supercritical CO_2 into a low pressure gas reservoir1. *Petrophysics* - The SPWLA Journal of Formation Evaluation and Reservoir Description, **50(04)**.

Mohammed, K. and P. Corbett (2003). How many relative permeability measurements do you need? A case study from a North African reservoir. *Petrophysics* - The SPWLA Journal of Formation Evaluation and Reservoir Description, **44(04)**.

Movchan, I.B., Shaygallyamova, Z.I., Yakovleva, A.A. and A.B. Movchan (2021). Increasing resolution of seismic hazard mapping on the example of the north of middle Russian highland. *Applied Sciences,* **11(11):** 5298.

Nygård, R., Gutierrez, M., Bratli, R.K. and K. Høeg (2006). Brittle-ductile transition, shear failure and leakage in shales and mudrocks. *Marine and Petroleum Geology,* **23(2):** 201-212.

Rücker, M., Bartels, W.B., Bultreys, T., Boone, M., Singh, K., Garfi, G., Scanziani, A., Spurin, C., Yesufu-Rufai, S., Krevor, S., Blunt, M.J., Wilson, O., Mahani, H., Cnudde, V., Luckham, P.F., Georgiadis, A. and S. Berg (2020). Workflow for upscaling wettability from the nanoscale to core scale. *Petrophysics* - The SPWLA Journal of Formation Evaluation and Reservoir Description, **61(02):** 189-205.

Sabah, M., Mehrad, M., Ashrafi, S.B., Wood, D.A. and S. Fathi (2021). Hybrid machine learning algorithms to enhance lost-circulation prediction and management in the Marun oil field. *Journal of Petroleum Science and Engineering*, **198:** 108125.

Worthington, P.F. (2010). Petrophysical evaluation of gas-hydrate formations. *Petroleum Geoscience,* **16(1):** 53-66.

Zhai, X., Chen, H., Lou, Y. and H. Wu (2021). Prediction and control model of shale induced fracture leakage pressure. *Journal of Petroleum Science and Engineering*, **198:** 108186.

Asian Journal of Water, Environment and Pollution

Volume 18 Number 4 **October – December, 2021**

Contents